Sensors and Actuators B 197 (2014) 370–375

Contents lists available at ScienceDirect

Sensors and Actuators B: Chemical

journal homepage: www.elsevier.com/locate/snb

Porous nanoplate-assembled CdO/ZnO composite microstructures: A highly sensitive material for ethanol detection

Li-Jing Zhou, Chunguang Li, Xiaoxin Zou**, Jun Zhao, Pan-Pan Jin, Liang-Liang Feng, Mei-Hong Fan, Guo-Dong Li*

State Key Laboratory of Inorganic Synthesis and Preparative Chemistry, College of Chemistry, Jilin University, Changchun 130012, PR China

ARTICLE INFO

Article history:
Received 11 December 2013
Received in revised form 24 February 2014
Accepted 25 February 2014
Available online 6 March 2014

Keywords:
ZnO
CdO
Nanocomposite
Gas sensor
Ethanol

ABSTRACT

Hierarchical CdO/ZnO composite materials composed of porous nanoplates are prepared by simple thermal treatment of a "pre-synthesized" cadmium–zinc bimetallic carbonate precursor. The gas-sensing properties of the as-synthesized nanocomposites are evaluated by a range of gases and organic vapors, and the results show that the gas sensors based on CdO/ZnO nanocomposites exhibit the highest sensing response towards ethanol relative to other testing gases. The optimal ratio of CdO to ZnO in CdO/ZnO nanocomposites is 7.5:100 for ethanol detection. The highest response of CdO/ZnO is ~7 and 59 times as high as those of the pure ZnO and the pure CdO, respectively. The significantly enhanced sensing performance of the CdO/ZnO nanocomposite is attributed to its novel hierarchical structure and synergetic effect between CdO and ZnO. In addition, the CdO/ZnO sensor exhibits short response and recovery times (<10 s) and a wide response range from 0.5 to 500 ppm for ethanol detection. In the testing range from 0.5 to 500 ppm, the logarithm of sensitivity shows a good linear dependency on the logarithm of ethanol concentration, indicating that the CdO/ZnO sensor may be used for quantitative detection of ethanol vapor.

1. Introduction

Accurate detection of flammable, explosive and/or toxic gases, especially at a low concentration, is of high importance to avoid some relevant serious accidents [1–4]. Practical gas detection relies on effective gas sensors, one of which is semiconductor-based one. The semiconductor-based sensors possess many inherent advantages, such as low cost, high stability and portability; and what is more, their fundamental mechanism is based on the gas-induced resistance variation of the semiconducting material. Zinc oxide (ZnO)—an important n-type wide-band gap semiconductor—is one of the first generation of sensing materials [1]. Since the discovery of ZnO's gas-sensing property, great efforts have been made to improve the performance of ZnO sensors, such as enhancing sensitivity and selectivity. One of the popular strategies is nanostructuring the ZnO sensing materials. Reducing the crystallite size down to the nanometer scale can significantly increase the surface area as well as surface reactive sites, and thereby can improve the gas-sensing properties (versus bulk ZnO). However, when nanosized ZnO material has to be used in a thin film form in sensing applications and worked at a high temperature (typically above 200 °C), their uncontrolled agglomeration would offset the nano effects to a certain extent. In order to minimize the uncontrolled agglomeration, it is feasible to pre-organize ZnO nanoparticles into a microsized structure, finally resulting into a hierarchical nanomaterial [5–17]. In this regard, there have already been some synthetic schemes for this kind of ZnO nanomaterials [5–17]. Most of the existing synthetic strategies are based on precursor-mediated solid-state conversion reactions, by which the obtained ZnO products can readily inherit the hierarchical nanostructure features of the solid precursors. The widely-used solid precursors are zinc-based carbonates, the hierarchical structure of which usually has to be formed with the help of some special additives such as polyvinyl pyrrolidone (PVP), hexamethylenetetramine, block copolymer F127 (EO106-PO70-EO106) and cetyltrimethylammonium bromide (CTAB) [5–12].

Herein we report a facile precursor-mediated synthetic route to porous nanoplate-assembled CdO/ZnO composite materials in the absence of any templates or additives. The as-obtained nanocomposite can serve as a highly sensitive material for the selective ethanol detection, thanks to its novel hierarchical structure and synergetic effect between CdO and ZnO (Note that CdO itself is a

* Corresponding author. Tel.: +86 431 85168318; fax: +86 431 85168624.
** Corresponding author.
E-mail addresses: chemistryzouxx@gmail.com (X. Zou), lgd@jlu.edu.cn, lifind@21cn.com (G.-D. Li).

http://dx.doi.org/10.1016/j.snb.2014.02.086
0925-4005/

low sensitive material [18–22]). This method involves controlled synthesis of Cd(II)–Zn(II) bimetallic carbonates (denoted as CZBC) as precursors, followed by a simple thermal treatment in air to form the CdO/ZnO composite materials. In particular, the CdO/ZnO composite with a Cd:Zn molar ratio of 7.5:100 was found to have the highest response to ethanol. Hereafter, CZBC and CdO/ZnO denote the product with this optimal composition (Cd:Zn = 7.5:100) if not particularly indicated. To the best of our knowledge, there were no reports on the synthesis of CdO/ZnO composite with hierarchical nanostructure previously. Notably also, this CdO/ZnO composite nanomaterial is among the most sensitive ZnO- and CdO-based ethanol sensing materials.

2. Experimental

2.1. Synthesis of CZBC and CdO/ZnO composites.

The CZBC precursor used herein was prepared in an ethylene glycol–water mixed solvent system, which was also used previously for the synthesis of other metal oxide/hydroxide nanostructures [23–25]. For the synthesis of CZBC (molar ratio Cd:Zn = 7.5:100), 5 mmol $Zn(NO_3)_2{\cdot}6H_2O$ and 2 mL $NH_3{\cdot}H_2O$ (25–28 wt.%) were added into an ethylene glycol–water mixed solvent (v/v = 1:1, 25 mL) to form solution 1; and 0.375 mmol $Cd(NO_3)_2{\cdot}4H_2O$ and 1 mL $NH_3{\cdot}H_2O$ (25–28 wt.%) were added into an ethylene glycol–water mixed solvent (v/v=1:1, 25 mL) to form solution 2. Solutions 1 and 2 were mixed under stirring and then 5 mmol Na_2CO_3 was added into the resulting mixture. The resulting mixture was put into a 100 mL Teflon-sealed autoclave, which was then heated at 80–180 °C for 10 h. The white precipitate (i.e., CZBC) was obtained after the autoclave was cooled to room temperature naturally. Next, the CZBC sample was thermally treated at 400 °C in air for 3 h, resulting in the formation of CdO/ZnO with a hierarchical structure. By varying the mole of $Cd(NO_3)_2{\cdot}4H_2O$ to $Zn(NO_3)_2{\cdot}6H_2O$ and keeping the rest of reaction procedures the same, various CdO/ZnO composite materials with different Cd:Zn ratios were obtained.

2.2. General characterization

The powder x-ray diffraction (XRD) patterns were recorded on a Rigaku D/Max 2550 x-ray diffractometer using CuKα radiation (λ = 1.5418 Å) operated at 200 mA and 50 kV. The scanning electron microscopic (SEM) images were taken on a JEOL JSM 6700F electron microscope. The transmission electron microscopy (TEM) and high-resolution TEM (HRTEM) images were obtained on a Philips-FEI Tecnai G2S-Twin with a field emission gun operating at 200 kv. The Brunauer–Emmett–Teller surface areas and Nitrogen adsorption–desorption isotherms of the samples were measured by using a Micromeritics ASAP 2020M system. The infrared (IR) spectra were recorded on a Bruker IFS 66V/S FTIR spectrometer using KBr pellets. The thermal gravimetric analysis curve was recorded on a NETZSCH STA 449C TG thermal analyzer from 25 to 800 °C at a heating rate of 10 °C/min in air. The x-ray photoelectron spectroscopy (XPS) was performed on an ESCALAB 250 x-ray photoelectron spectrometer with a monochromated x-ray source (Al Kα $h\upsilon$ = 1486.6 eV).

2.3. Sensor fabrication and testing

The gas sensor was fabricated by pasting viscous slurry of the obtained sample onto an alumina tube with a diameter of 1 mm and a length of 4 mm, which was positioned with a pair of Au electrodes and four Pt wires on both ends of the tube. A Ni–Cr alloy coil passing through the tube was employed as a heater to control the operating temperature. The schematic structure of the sensor is shown in Fig. 1 [23]. For comparison, all of the sensors were fabricated using the same method, and only the difference may be the CdO/ZnO ratio in the material. Gas sensing tests were performed on a commercial CGS-8 Gas Sensing Measurement System (Beijing Elite Tech Company Limited).

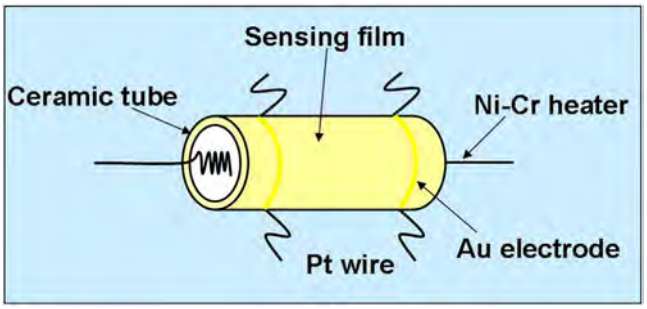

Fig. 1. A diagram of the sensor structure.

Gas sensing properties were measured using a static test system which included a test chamber (~1 L in volume) at room temperature (~25 °C). Environmental air with a relative humidity of ~30% was used as both a reference gas and a diluting gas to obtain the desired concentrations of target gases. A typical testing procedure was as follows. After the target gas was injected into the test chamber for about 5 min by a syringe, the sensor was put into the test chamber. When the response reached a constant value, the sensor was taken out to recover in fresh air. The sensor response is defined as the ratio of R_a to R_g, where R_a and R_g are the electrical resistance of the sensor in atmospheric air and in the testing gas, respectively.

3. Results and discussion

The structure of CZBC was studied by powder x-ray diffraction (XRD) shown in Fig. S1, ESI†, and it is clear that the CZBC precursor contains $Zn_5(OH)_6(CO_3)_2$ (JCPDS 19-1458) and $CdCO_3$ (JCPDS 42-1342). The structure and composition of CZBC were further confirmed by FT-IR spectroscopy (Fig. S2, ESI†) and thermal gravimetric analysis (TG, Fig. S3, ESI†). In Fig. S2, ESI†, the broad IR absorption band centered at ~3317 cm^{-1} can be attributed to hydroxyl group and absorbed water. The intense sharp peaks at 1507 and 1387 cm^{-1} are attributed to the ν_3 mode of the CO_3^{2-} group, and the 834 and 710 cm^{-1} are assigned to ν_2 and ν_4 mode of the CO_3^{2-} group, respectively. These IR results further confirm that CZBC contains metal carbonates. In Fig. S3, ESI†, TG analysis of CZBC was carried out in air from 25 to 800 °C. With the increase of temperature from 25 to 800 °C, the weight loss starts at 250 °C and reaches a constant at about 400 °C. This weight loss is originated from the decomposition of metal carbonates (i.e., CZBC). For comparative purpose, two more samples were synthesized by using only Zn^{2+} or Cd^{2+} ions under the same synthetic condition of CZBC. The resulting monometallic materials were well indexed (Fig. S1, ESI†) to $Zn_5(OH)_6(CO_3)_2$ and $CdCO_3$; and they were correspondingly denoted here as ZMC and CMC, respectively.

The morphology of the CZBC precursor was observed by scanning electron microscopy (SEM). The low-magnification SEM images (Fig. 2A) show that the product consists of nearly spherical particles with a diameter of 1–4 μm. The more detailed structural feature of CZBC was shown in the high-magnification SEM image (Fig. 2B). It is clearly seen that the surface of a single CZBC particle is composed of densely packed plate-like subunits with a thickness of 20–40 nm. In addition, ZMC (without Cd) also possesses a nanoplate-assembled hierarchical structure, whereas CMC (without Zn) only gives an irregular nanoparticle shape (Fig. S4, ESI†). In addition, Cd(II)–Zn(II) bimetallic carbonates with the Cd:Zn atomic ratio of 2.5:100, 5:100 and 10:100 were also prepared under the

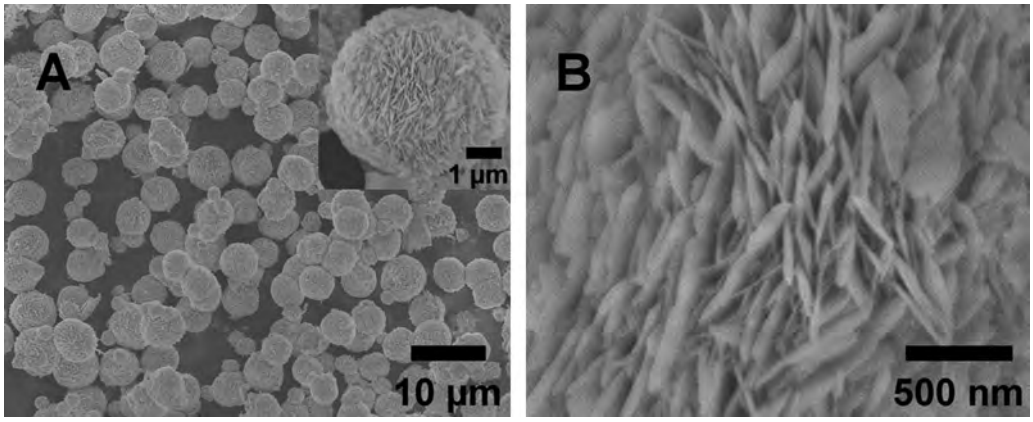

Fig. 2. SEM images of the CZBC precursor.

same synthetic condition of CZBC. All of these samples have a nanoplate-assembled hierarchical structure (Fig. S5, ESI†), which is similar to that of CZBC. From the above results, it can be concluded that the hierarchical structure of CZBC would be mainly controlled by the self-assembly of $Zn_5(OH)_6(CO_3)_2$, and a small amount of $CdCO_3$ could co-assemble with $Zn_5(OH)_6(CO_3)_2$. We also found that the enough amount of Na_2CO_3 and the presence of ethylene glycol are important for the formation of the CZBC precursor with a hierarchical structure (Fig. S6 and 7, ESI†). The enough amount (>2.4 mmol) of Na_2CO_3 in the reaction system is necessary to ensure that all the metal ions (i.e., Zn^{2+} and Cd^{2+}) finally can be converted into metal carbonates (Fig. S6, ESI†), and the presence of ethylene glycol in the reaction system was found to be helpful for the assembly of nanosheets (Fig. S7, ESI†).

Through a simple thermal treatment process at 400 °C, the CZBC precursor was directly converted into CdO/ZnO composite. For comparison, pure CdO and pure ZnO samples were also synthesized by thermal treatment of CMC and ZMC at 400 °C, respectively. Fig. 3 shows the XRD patterns of the as-obtained CdO/ZnO, CdO, ZnO samples. It is seen that the XRD peaks associated with the CZBC precursor (Fig. S1, ESI†) completely disappear upon calcination, and some new diffraction peaks, which are perfectly indexed to hexagonal ZnO (JCPDS 36-1451) and cubic CdO (JCPDS 65-2908), show up in the XRD pattern of CdO/ZnO. Although there is no obvious shift of CdO/ZnO's XRD peaks relative to those of pure ZnO and pure CdO by using KCl as internal standard (Fig. S8, ESI†), it is still possible that trace Cd^{2+} ions are doped into the ZnO crystal lattice, and/or trace Zn^{2+} ions are doped into the CdO crystal lattice, especially at the interface of ZnO and CdO nanocrystals. The conversion of CZBC to CdO/ZnO was also confirmed by IR analysis (Fig. S9, ESI†), because those IR absorption bands related to CO_3^{2-} in CZBC (Fig. S2, ESI†) are not observed in the IR spectrum of CdO/ZnO.

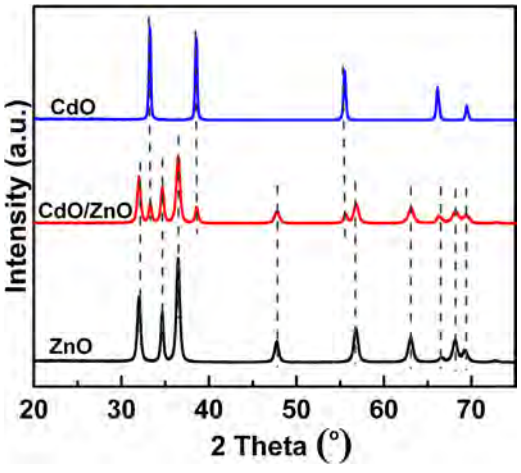

Fig. 3. XRD patterns of pure ZnO, pure CdO and CdO/ZnO derived from ZMC, CMC and CZBC, respectively.

Fig. 4A shows typical SEM images of CdO/ZnO. The SEM images reveal that CdO/ZnO maintains the morphology, size and plate-like nanosized building blocks of the CZBC precursor. Different from the CZBC precursor with nonporous nanoplates as building blocks, the CdO/ZnO material possesses loosely-packed nanoplates with an observable porous structure. The pore size is in the range of 10–20 nm. From CZBC to CdO/ZnO, the change of their basic building blocks is attributed to the thermal-driven decomposition of metal carbonates (i.e., CZBC) and thereby there are some structural contractions during the thermal treatment process. The TEM image of CdO/ZnO's fragments (Fig. 5A) further confirms the porous structure of the nanoplates in CdO/ZnO. Moreover, elemental-mapping of the CdO/ZnO material (Fig. 4B–E) shows that all the elements, i.e., Cd, Zn, and O, were homogeneously distributed over the entire CdO/ZnO microparticle. The high-resolution transmission electron microscopy (HRTEM) image (Fig. 5B) of the sample clearly shows the junction of ZnO nanoparticle and CdO nanoparticle. These results further confirm that the CdO and ZnO nanocrystals were well dispersed within the obtained CdO/ZnO material.

The N_2 adsorption–desorption isotherms of CdO/ZnO (Fig. S10A, ESI†) exhibit a characteristic type-IV isotherm with an H3 hysteresis loop, indicating the presence of mesoporous/macroporous structure in the material. The corresponding BJH pore-size distribution (Fig. S10B, ESI†) derived from desorption branch of the isotherm shows a wide pore-size distribution ranging from 2 to 70 nm, further confirming the existence of mesopores and macropores in the material. This result is also in agreement with the SEM and TEM observations. The corresponding BET surface area of this material is about 24 $m^2\ g^{-1}$.

Due to the importance of ethanol sensors in food control applications [5–17], the sensing performance of the CdO/ZnO nanocomposite material was evaluated by using ethanol as the testing gas. The response and recovery time of the sensor are defined as the times taken by the sensor to achieve 90% of the total resistance change. The optimal operating temperature of the CdO/ZnO sensor was determined by testing 100 ppm ethanol, and the result shows that the optimal operation temperature is around 240 °C (Fig. 6). This value is within the scope of temperatures that are usually required to make the semiconductor-based sensors work well [1].

Fig. 7A shows the sensing performances of various CdO/ZnO samples with different CdO:ZnO mol ratios, from which the following conclusions can be made. (1) Pristine ZnO (without CdO) is

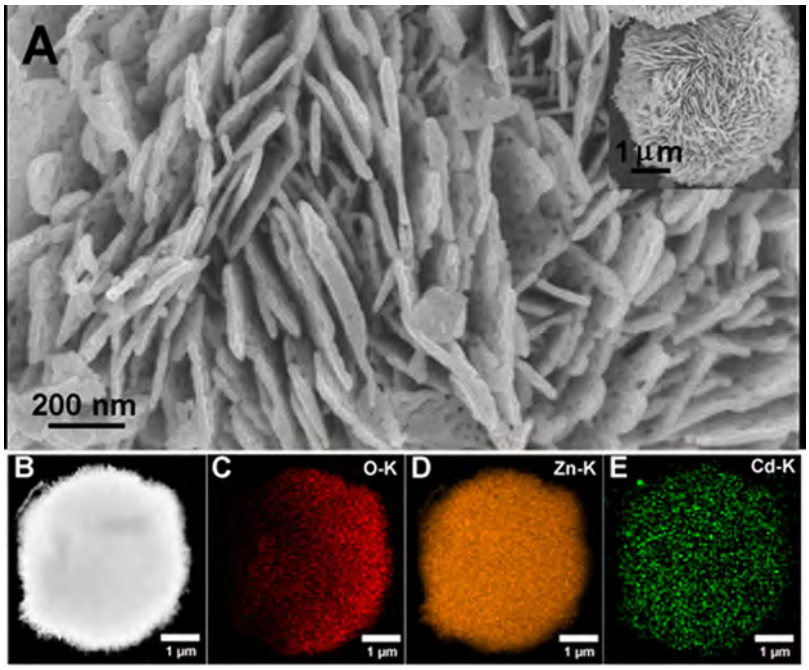

Fig. 4. (A) SEM images, (B) scanning transmission electron microscope (STEM) image and (C–E) the corresponding elemental mapping images of CdO/ZnO.

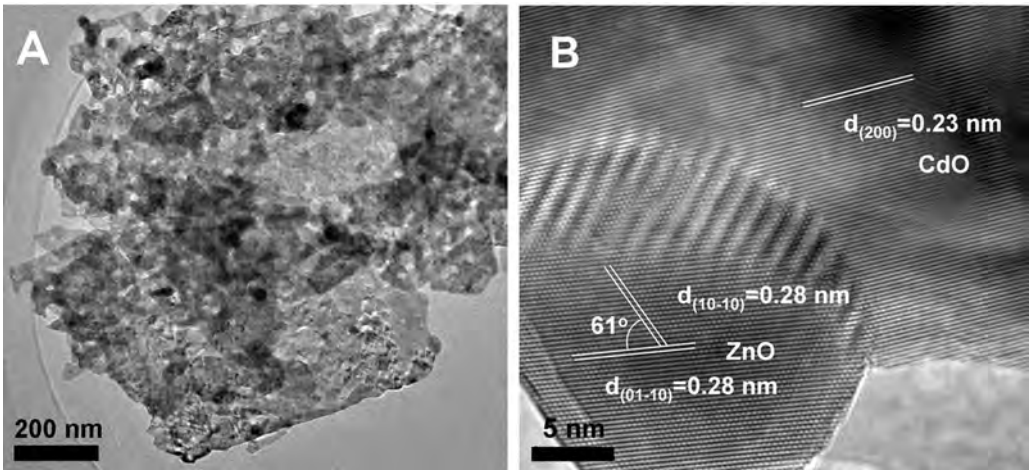

Fig. 5. TEM image (A) and HRTEM image (B) of CdO/ZnO.

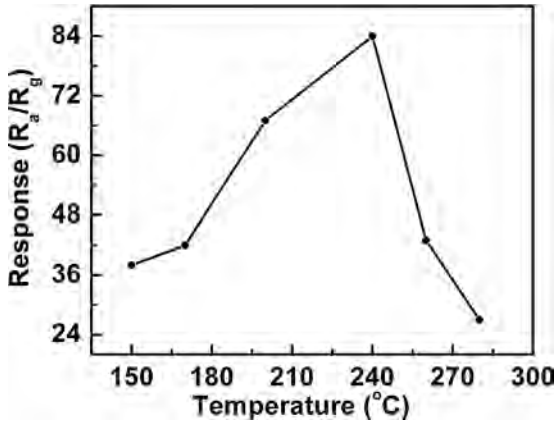

Fig. 6. Response of the sensor based on the CdO/ZnO sample as a function of the operating temperature for the detection of ethanol with a concentration of 100 ppm.

more sensitive towards ethanol than pristine CdO (without ZnO). The response of the former is about 8.5 times higher than that of the latter. This indicates that the ZnO are mainly responsible for the sensing performance of CdO/ZnO, with the CdO rendering cooperative effects. (2) CdO significantly improves the ZnO's response for ethanol detection, with the one with CdO:ZnO = 7.5:100 exhibiting the highest sensitivity. The response of CdO/ZnO sensor is ~7 times as high as that of the pure ZnO sensor. Also noteworthy, our CdO/ZnO nanomaterial is among the most sensitive ZnO-, CdO-based and other ethanol sensing materials (see Table S1 and Table S2 in ESI†) [26–32].

Fig. 7B shows the typical dynamic response–recovery curve of the CdO/ZnO sensor with increasing ethanol concentrations. It is seen that the sensor has a wide response range of 0.5–500 ppm for ethanol detection. The response increases significantly with the increase of ethanol concentration. Moreover, the response is about 1.3 at an ethanol concentration of 0.5 ppm, and thus the detection limit of the CdO/ZnO sensor can be said to be 0.5 ppm, which is much lower than that (2 ppm) of the commercial ZnO sensor. In

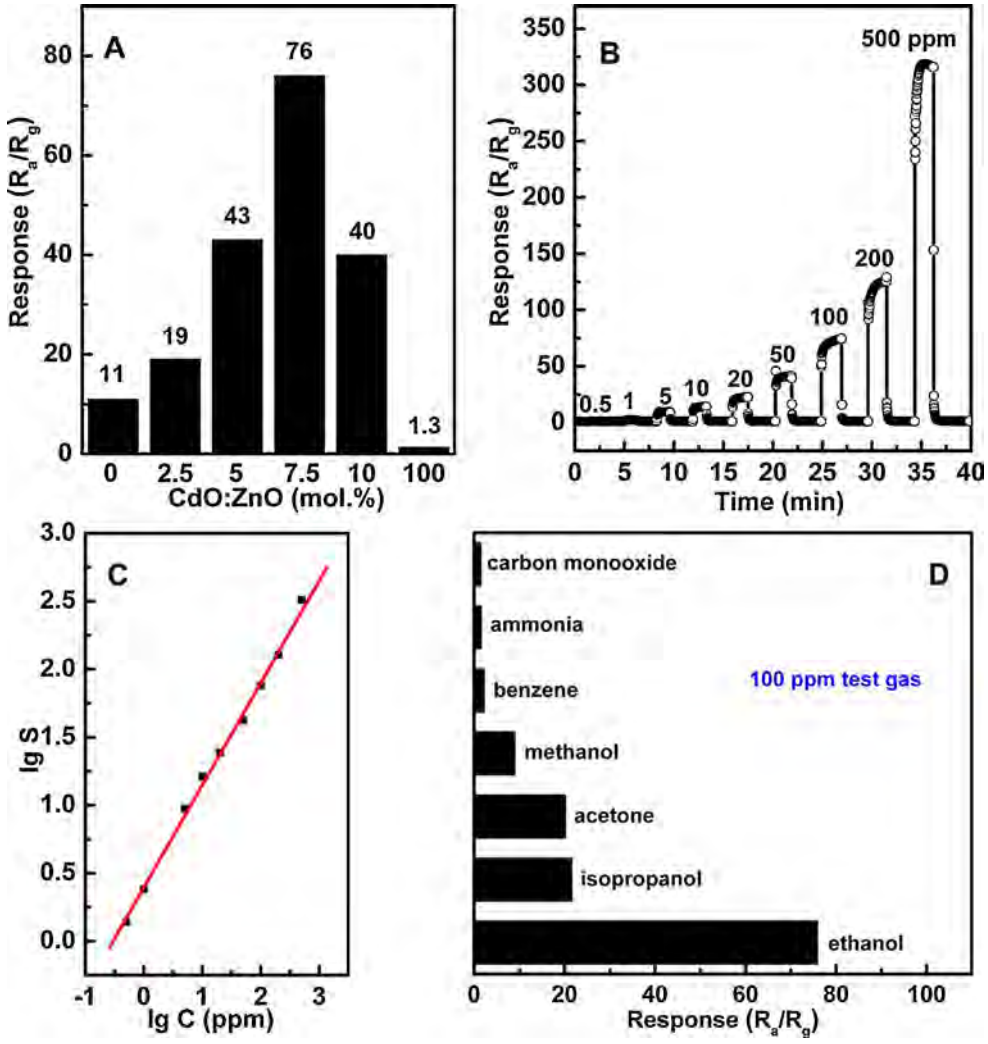

Fig. 7. (A) Response of a series of CdO/ZnO samples with different CdO:ZnO mol ratios (evaluated in presence of 100 ppm ethanol); (B) dynamic response–recovery curves of the sensor based on CdO/ZnO for ethanol detection; (C) variation of sensitivity (S) of the CdO/ZnO sensor with ethanol concentration (ppm); and (D) response of the CdO/ZnO sensor in the presence of different test gases (100 ppm).

the testing range from 0.5 to 500 ppm, the logarithm of sensitivity shows a good linear dependency on the logarithm of ethanol concentration (Fig. 7C), indicating that the CdO/ZnO sensor may be used for quantitative detection of ethanol vapor. In addition, the CdO/ZnO sensor exhibits fast response and recovery time (<10 s). The sensing performance of the CdO/ZnO sensor was further investigated by testing a wide range of gases and organic vapors (Fig. 7D). It is obvious that the CdO/ZnO sensor is more sensitive to ethanol than other gases/vapors including isopropanol, methanol, acetone, benzene, ammonia and carbon monoxide. Nevertheless, further investigation may still be required to improve the selectivity of the material via surface modification with noble metal particles and bulk doping with heteroatoms.

It is well known that ZnO is an n-type wide bandgap semiconductor, and its gas sensing behavior is generally explained based on the interaction of surface chemisorbed oxygen species and the gas molecules to be detected [1]. First, ZnO as an n-type semiconductor can absorb oxygen molecules in air. The chemisorbed oxygen molecules on the ZnO surface can function as electron acceptors to extract electrons from the conduction band of ZnO. This will lead to the creation of a potential barrier and thus a high resistance state. Next, when the ZnO sensor is exposed to a target gas (such as ethanol) at the operation temperature, the target gas will react with the oxygen species on the ZnO surface. This will result in the decrease of the chemisorbed oxygen's amount, the reduction of the potential barrier's height, and thereby the decrease of the sensor's resistance.

Based on the ZnO's sensing mechanism described above as well as the CdO's properties, two possible reasons are proposed to explain why CdO can improve the sensing performance of ZnO. (1) CdO is a low electrical resistivity material [33–35], and thereby it would decrease the resistance of the CdO/ZnO composite material. This would enable the easy detection of the resistance variation during the sensing measurement and the rapid electron transportation between the electrodes of the sensor [36–38]. (2) CdO is an n-type semiconductor with a large amount of native oxygen vacancies (this is also the reason why CdO possesses a low resistance) [18–21,33–35]. This property would be helpful to the adsorption of oxygen molecules on the surface of the CdO/ZnO composite; and the increase in amount of surface chemisorbed oxygen should be beneficial to the surface reaction activity/kinetics, and thereby enhanced sensing properties [36].

4. Conclusions

In summary, we reported the synthesis of hierarchical CdO/ZnO nanocomposite material, which was used as an efficient sensing material for ethanol detection. The significantly enhanced sensing

performance of the CdO/ZnO nanocomposite is attributed to its novel hierarchical structure and synergetic effect between CdO and ZnO. We believe that this study would further promote the exploitation of semiconductor nanocomposite for gas sensors.

This work was supported by the National Natural Science Foundation of China (21371070).

References

[1] M.E. Franke, T.J. Koplin, U. Simon, Metal and metal oxide nanoparticles in chemiresistors: does the nanoscale matter? Small 2 (2006) 36–50.
[2] M.D. Arienzo, L. Armelao, C.M. Mari, S. Polizzi, R. Ruffo, R. Scotti, F. Morazzoni, Macroporous WO_3 thin films active in NH_3 sensing: role of the hosted Cr isolated centers and Pt nanoclusters, J. Am. Chem. Soc. 133 (2011) 5296–5304.
[3] X.X. Zou, G.D. Li, J. Zhao, P.P. Wang, Y.N. Wang, L.J. Zhou, J. Su, L. Li, J.S. Chen, Light-driven transformation of ZnS-cyclohexylamine nanocomposite into zinc hydroxysulfate: a photochemical route to inorganic nanosheets, Inorg. Chem. 50 (2011) 9106–9113.
[4] L. Xu, R. Zheng, S. Liu, J. Song, J. Chen, B. Dong, H. Song, NiO@ZnO heterostructured nanotubes: coelectrospinning fabrication, characterization, and highly enhanced gas sensing properties, Inorg. Chem. 51 (2012) 7733–7740.
[5] J. Li, H. Fan, X. Jia, Multilayered ZnO nanosheets with 3D porous architectures: synthesis and gas sensing application, J. Phys. Chem. C 114 (2010) 14684–14691.
[6] L. Zhang, J. Zhao, H. Lu, L. Li, J. Zheng, H. Li, Z. Zhu, Facile synthesis and ultrahigh ethanol response of hierarchically porous ZnO nanosheets, Sens. Actuators, B 161 (2012) 209–215.
[7] Z.H. Jing, J.H. Zhan, Fabrication and gas-sensing properties of porous ZnO nanoplates, Adv. Mater. 20 (2008) 4547–4551.
[8] J. Zhang, S.R. Wang, M.J. Xu, Y. Wang, B.L. Zhu, S.M. Zhang, W.P. Huang, S.H. Wu, Hierarchically porous ZnO architectures for gas sensor application, Cryst. Growth Des. 9 (2009) 3532–3537.
[9] Y.C. Qiu, W. Chen, S.H. Yang, Facile hydrothermal preparation of hierarchically assembled, porous single crystalline ZnO nanoplates and their application in dye-sensitized solar cells, J. Mater. Chem. 20 (2010) 1001–1006.
[10] X.H. Liu, J. Zhang, L.W. Wang, T.L. Yang, X.Z. Guo, S.H. Wu, S.R. Wang, 3D hierarchically porous ZnO structures and their functionalization by Au nanoparticles for gas sensors, J. Mater. Chem. 21 (2011) 349–356.
[11] X.Z. Wang, W. Liu, J.R. Liu, F.L. Wang, J. Kong, S. Qiu, C.Z. He, L.Q. Luan, Synthesis of nestlike ZnO hierarchically porous structures and analysis of their gas sensing properties, ACS Appl. Mater. Interf. 4 (2012) 817–825.
[12] H.J. Zhang, R.F. Wu, Z.W. Chen, G. Liu, Z.N. Zhang, Z. Jiao, Self-assembly fabrication of 3D flower-like ZnO hierarchical nanostructures and their gas sensing properties, CrystEngComm 14 (2012) 1775–1782.
[13] K.M. Kim, H.R. Kim, K.I. Choi, H.J. Kim, J.H. Lee, ZnO hierarchical nanostructures grown at room temperature and their C_2H_5OH sensor applications, Sens. Actuators, B 155 (2011) 745–751.
[14] J. Zhao, X.X. Zou, L.J. Zhou, L.L. Feng, P.P. Jin, Y.P. Liu, G.D. Li, Precursor-mediated synthesis and sensing properties of wurtzite ZnO microspheres composed of radially aligned porous nanorods, Dalton Trans. 42 (2013) 14357–14360.
[15] Y. Zhang, J.Q. Xu, Q. Xiang, H. Li, Q.Y. Pan, P.C. Xu, Brush-like hierarchical ZnO nanostructures: synthesis, photoluminescence and gas sensor properties, J. Phys. Chem. C 113 (2009) 3430–3435.
[16] B. Liu, J. Xu, S.H. Ran, Z.R. Wang, D. Chen, G.Z. Shen, High-performance photodetectors, photocatalysts, and gas sensors based on polyol reflux synthesized porous ZnO nanosheets, CrystEngComm 14 (2012) 4582–4588.
[17] P.P. Wang, Q. Qi, X.X. Zou, J. Zhao, R.F. Xuan, G.D. Li, A precursor route to porous ZnO nanotubes with superior gas sensing properties, RSC Adv. 3 (2013) 23980–23983.
[18] A.S. Kamble, R.C. Pawar, N.L. Tarwal, L.D. More, P.S. Patil, Ethanol sensing properties of chemosynthesized CdO nanowires and nanowalls, Mater. Lett. 65 (2011) 1488–1491.
[19] D.S. Raja, T. Krishnakumar, R. Jayaprakash, T. Prakash, G. Leonardi, G. Neri, CO sensing characteristics of hexagonal-shaped CdO nanostructures prepared by microwave irradiation, Sens. Actuators, B 171-172 (2012) 853–859.
[20] D. Sivalingam, J.B. Gopalakrishnan, J.B. Rayappan, Nanostructured mixed ZnO and CdO thin film for selective ethanol sensing, Mater. Lett. 77 (2012) 117–120.
[21] N. Han, X.F. Wu, D.W. Zhang, G.L. Shen, H.D. Liu, Y.F. Chen, CdO activated Sn-doped ZnO for highly sensitive, selective and stable formaldehyde sensor, Sens. Actuators, B 152 (2011) 324–329.
[22] P. Hu, N. Han, D.W. Zhang, J.C. Ho, Y.F. Chen, Highly formaldehyde-sensitive, transition-metal doped ZnO nanorods prepared by plasma-enhanced chemical vapor deposition, Sens. Actuators, B 169 (2012) 74–80.
[23] L.J. Zhou, Y.C. Zou, J. Zhao, P.P. Wang, L.L. Feng, L.W. Sun, D.J. Wang, G.D. Li, Facile synthesis of highly stable and porous Cu_2O/CuO cubes with enhanced gas sensing properties, Sens. Actuators, B 188 (2013) 533–539.
[24] S.W. Cao, Y.J. Zhu, J. Chang, Fe_3O_4 polyhedral nanoparticles with a high magnetization synthesized in mixed solvent ethylene glycol–water system, New J. Chem. 32 (2008) 1526–1530.
[25] S. Ashoka, G. Nagaraju, C.N. Tharamani, G.T. Chandrappa, Ethylene glycol assisted hydrothermal synthesis of flower like ZnO architectures, Mater. Lett. 63 (2009) 873–876.
[26] L.X. Zhang, J.H. Zhao, H.Q. Lu, L. Li, J.F. Zheng, H. Li, Z.P. Zhu, Facile synthesis and ultrahigh ethanol response of hierarchically porous ZnO nanosheets, Sens. Actuators, B 161 (2012) 209–215.
[27] Y.J. Chen, C.L. Zhu, G. Xiao, Reduced-temperature ethanol sensing characteristics of flower-like ZnO nanorods synthesized by a sonochemical method, Nanotechnology 17 (2006) 4537.
[28] L.X. Zhang, Y.Y. Yin, Large-scale synthesis of flower-like ZnO nanorods via a wet-chemical route and the defect-enhanced ethanol-sensing properties, Sens. Actuators, B 183 (2013) 110–116.
[29] K.M. Kim, H.R. Kim, K. Choi, H.J. Kim, J.H. Lee, ZnO hierarchical nanostructures grown at room temperature and their C_2H_5OH sensor applications, Sens. Actuators, B 155 (2011) 745–751.
[30] S.J. Kim, I.S. Hwang, J.K. Choi, Y.C. Kang, J.H. Lee, Enhanced C_2H_5OH sensing characteristics of nano-porous In_2O_3 hollow spheres prepared by sucrose-mediated hydrothermal reaction, Sens. Actuators, B 155 (2011) 512–751.
[31] L.J. Guo, X.P. Shen, G.X. Zhu, K.M. Chen, Preparation and gas-sensing performance of In_2O_3 porous nanoplatelets, Sens. Actuators, B 155 (2011) 752–758.
[32] S.Q. Liu, M.J. Xie, Y.X. Li, X.F. Guo, W.J. Ji, W.P. Ding, C.T. Au, Novel sea urchin-like hollow core–shell SnO_2 superstructures: facile synthesis and excellent ethanol sensing performance, Sens. Actuators, B 151 (2010) 229–235.
[33] Y. Ding, Y. Wang, L.C. Zhang, H. Zhang, Y. Lei, Preparation, characterization and application of novel conductive NiO–CdO nanofibers with dislocation feature, J. Mater. Chem. 22 (2012) 980–986.
[34] Z.Y. Zhao, D.L. Morel, C.S. Ferekides, Electrical and optical properties of tin-doped CdO films deposited by atmospheric metalorganic chemical vapor deposition, Thin Solid Films 413 (2002) 203–211.
[35] M. Ocampo, A.M. Fernandez, P.J. Sebastian, Transparent conducting CdO films formed by chemical bath deposition, Semicond. Sci. Technol. 18 (1993) 750–751.
[36] J. Su, X.X. Zou, Y.C. Zou, G.D. Li, P.P. Wang, J.S. Chen, Porous titania with heavily self-doped Ti^{3+} for specific sensing of CO at room temperature, Inorg. Chem. 52 (2013) 5924–5930.
[37] G.H. Lu, L.E. Ocola, J.H. Chen, Room-temperature gas sensing based on electron transfer between discrete tin oxide nanocrystals and multiwalled carbon nanotubes, Adv. Mater. 21 (2009) 2487–2491.
[38] A. Yang, X.M. Tao, R.X. Wang, S.C. Lee, C. Surya, Room temperature gas sensing properties of SnO_2/multiwall-carbon-nanotube composite nanofibers, Appl. Phys. Lett. 91 (2007) 133110.

Biographies

Li-Jing Zhou received her B.Sc. chemistry degree from Heibei North University, China, in 2009. Presently, she is a PhD student at State Key Laboratory of Inorganic Synthesis & Preparative Chemistry, Jilin University in China.

Chunguang Li is an engineer at State Key Laboratory of Inorganic Synthesis & Preparative Chemistry, Jilin University in China. Her research interest lies in inorganic materials and their structures.

Xiaoxin Zou was awarded a Ph.D. in Inorganic Chemistry from Jilin University (China) in 06/2011; and then moved to the University of California, Riverside and Rutgers, The State University of New Jersey as a Postdoctoral Scholar from 07/2011 to 10/2013. He is currently an associate professor in Jilin University. His research interests focus on the design and synthesis of noble metal-free, nanostructured and/or nanoporous materials for water splitting and renewable energy applications.

Jun Zhao received her B.Sc. chemistry degree from Changchun Institute of Technology, China, in 2006. She is currently undertaking her PhD at State Key Laboratory of Inorganic Synthesis & Preparative Chemistry, Jilin University in China.

Pan-Pan Jin is a master student at State Key Laboratory of Inorganic Synthesis & Preparative Chemistry, Jilin University in China. Her research interest is the synthesis of sensing nanomaterials.

Liang-Liang Feng is a PhD student at State Key Laboratory of Inorganic Synthesis & Preparative Chemistry, Jilin University in China. Her research interest is the synthesis of porous metal oxide materials.

Mei-Hong Fan received her B.S. degree from Department of Chemistry, Anyang Normal University in 2013. Now, she is a postgraduate student at State Key Laboratory of Inorganic Synthesis & Preparative Chemistry, Jilin University. She has majored in the synthesis of nanomaterials.

Guo-Dong Li is a full professor at State Key Lab of Inorganic Synthesis & Preparative Chemistry, College of Chemistry, Jilin University in China. He received his B.Sc. (1995), M.Sc (1998) and PhD (2001) from Jilin University. His research interests include chemical sensors, lithium batteries, photocatalysts.